ChemComm

ROYAL SOCIETY OF CHEMISTRY

COMMUNICATION

View Article Online
View Journal | View Issue



Cite this: *Chem. Commun.*, 2020, **56**, 8627

Received 30th April 2020,
Accepted 22nd June 2020

DOI: 10.1039/d0cc03122d

rsc.li/chemcomm



# Enhancement of the oxygen reduction reaction electrocatalytic activity of metallo-corroles using contracted cobalt(III) $CF_3$-corrole incorporated in a high surface area carbon support†

Hilah C. Honig, Ariel Friedman, Noam Zion and Lior Elbaz *

**Molecular oxygen reduction reaction catalysts based on metallo-corrole with the smallest *meso*-substituent reported to-date, Co(III)$CF_3$-corrole, was synthesized and compared to the well-studied Co(III)tpfcorrole when adsorbed on a high surface area carbon support. This study shows the improved electrocatalytic performance with the new corrole, attributed to its unique compact structure, which enables surface interactions in favor of lowering the reaction overpotential by 70 mV.**

The world's leading economies have come to realize that fossil fuels are not an everlasting resource, and that energy-related carbon dioxide emissions must be dropped significantly.[1] Among the various technologies available, low temperature fuel cells (LTFCs), namely: proton exchange membrane and alkaline electrolyte membrane fuel cells, seem to have the most promise for high power density applications such as transportation, backup and main power.[2] In order to increase the fuel cell's reaction rate, and lower the activation energy, electrocatalysts are needed.[3] The relatively sluggish kinetics of the oxygen reduction reaction (ORR) at the cathode results in a significant energy loss, and requires large amounts of catalysts.[4]

The most common ORR catalysts today are platinum-group metal (PGM) catalysts, which are scarce and account for the relatively high cost of LTFCs.[4,5] Moreover, PGMs are considered to be non-selective catalysts, and tend to accelerate the degradation of carbon-based electrodes.[6] For these reasons, the search for alternative, PGM-free catalysts has been increasing during the past couple of decades.[3] The work on this class of catalysts has been inspired by biological systems that reduce oxygen very efficiently, using transition metal complexes.[7,8] While the state-of-the-art PGM-free ORR catalysts are heat-treated mixtures of a first-row transition metal, nitrogen and carbon precursors (MNCs), their undefined structure limits their further improvement. Hence, the need for well-defined molecular catalysts is clear. We recently reported on the very promising activity of a family of molecular PGM-free ORR catalysts based on metallocorroles (Fig. 1).[6,9–17]

In the past few years, we have studied the parameters that affect the ORR electrocatalytic activity of metallo-corroles.[18] We concluded that in terms of overpotential and selectivity, the most active metal center is Co(III). In order to further lower the ORR overpotential, a wide array of substituents were studied, both at the beta and *meso* positions on the corrole ring, having different electronegativities, making them anywhere from very strong electron-donating to very strong electron-withdrawing substituents.[10,11,18] Although electron-withdrawing substituents lower the overpotential when used as is, after their incorporation in high surface area carbon, the effect of the nature of the substituent diminishes, and all of the studied metallo-corroles catalyze the ORR at the same potential. These findings led us to postulate that the metallo-corrole's substituents do not affect the ORR overpotential when these complexes are adsorbed on high surface area carbon supports. We now report on the activity of the smallest corrole structure reported to date, which enables the removal of the complexity

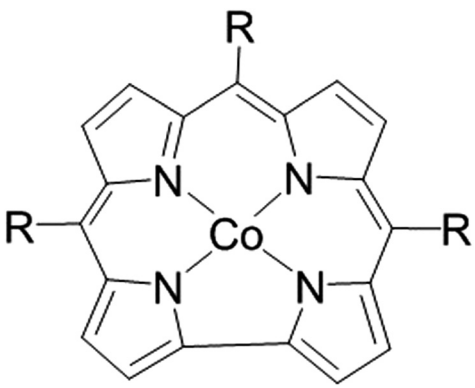


Fig. 1 The structure of Cobalt (III) corrole. $CF_3$-corrole R = $CF_3$ (trifluoromethyl), tpf-corrole R = $C_6F_5$ (tris-pentafluoro phenyl).

*Chemistry Department, Bar-Ilan University, Ramat-Gan, Israel.*
*E-mail: lior.elbaz@biu.ac.il*

† Electronic supplementary information (ESI) available: Experimental and XPS data. See DOI: 10.1039/d0cc03122d

and the bulkiness of other metallo-corroles, and is expected to be one of the most electrocatalytically active corroles.

In this work, a contracted cobalt-corrole containing only the $CF_3$ substituent on its *meso*-position was synthesized (see details in the SI†), and its ORR electrocatalytic activity was compared to that of Co(III) tri-(pentafluorophenyl)corrole (Co(III) tpf-corrole) (Fig. 1). It is expected that the compactness of this new corrole will increase its chance of forming favorable surface interactions with the carbon supports, as was previously shown with other catalysts,[19,20] while maintaining the already high activity associated with this family of molecular catalysts, and will allow the increase of the activity and catalytic site density of these PGM-free molecular catalysts; one of the biggest challenges in the field today.[21–23] Previous work with Co(III) $CF_3$-corrole showed that it tends to form a very stable axial coordination on the metal center, whereas more elaborate structures show limited-to-no stability.[24–26]

Both substituents ($CF_3$ and tpf) are considered very electronegative, and stabilize the corrole's ring.[11] And both significantly contribute to the electron-withdrawing tendency of the ring, which is important for lowering the ORR overpotential with transition metal complexes.[27,28] The ORR activity of these corroles when adsorbed on a high surface area carbon support, black pearls 2000 (BP2000), was studied in alkaline and acidic environments. Both exhibit very high activity in the alkaline environment, on par with the state-of-the-art molecular catalysts (Fig. 2). While in the acidic environment, they show a much lower activity (Fig. S2, ESI†). Hence, in this work, we focused on the performance in an alkaline environment.

As shown by the RRDE results (Fig. 2), the ORR activity of the $CF_3$-substituted corrole outperforms that of tpf-corrole in terms of reaction potentials. The onset and half-wave potentials for ORR with the $CF_3$-corrole are 0.89 and 0.83 V *vs.* RHE, respectively. The tpf-corrole has an onset potential of 0.85 V *vs.* RHE and a half-wave potential of 0.76 V *vs.* RHE. In contrast to other *meso*-substituted Co(III)-corroles that were studied in the past, which did not show a significant difference in their ORR potentials (Fig. S3, ESI†), the $CF_3$-substituted corrole's half-wave potential was significantly shifted to a lower overpotential by 70 mV, hinting at some new effect that was not observed before.[10]

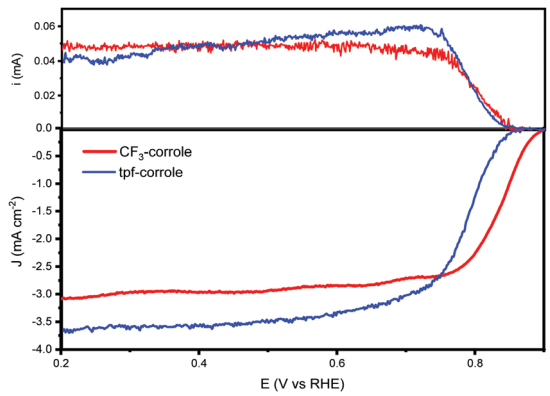


Fig. 2 RRDE of $CF_3$-corrole and tpf-corrole in 0.1 M KOH @ 900 rpm.

In order to understand the cause for the shift in ORR potentials, X-ray photoelectron spectroscopy (XPS) was used. Fig. 3 presents a summary of the XPS spectra of both corroles. The spectra before incorporation in BP2000 show one main O1s peak at 531.28 eV and 532.88 eV, for the $CF_3$- and tpf-corrole, respectively. These peaks can be assigned to a combination of various Co–O species, most probably an environmental oxygen adduct on the cobalt metal center in the corrole (Co–$O_2$).[29] This observation was confirmed by the Co2p spectra (Fig. 3, left). After the adsorption on BP2000, the O1s peak of pristine tpf-corrole shifted by 0.3 eV to 533.18 eV, while the peak of the $CF_3$-corrole was much more significantly shifted, by 2.0 eV to 533.28 eV. The fact that the peak of both pristine corroles shifted implies surface interactions with BP2000. It seems that these surface interactions are through the oxygen of the quinone-like moieties on the BP2000 surface, similar to previous observations with cobalt–porphyrins.[20,30] After the incorporation in BP2000, the Co2p peak of $CF_3$-corrole, at 780.08 eV, becomes significantly more dominant, implying the formation of a strong bond to the surface of BP2000 through the oxygen moieties. This is in agreement with the O1s spectra. In contrast, the tpf-corrole shows much weaker Co–O bonds after its incorporation in BP2000. These results are also in agreement with the stronger tendency of the $CF_3$-corrole for binding axial ligands.[24–26] Further computational study is needed in order to elucidate how these surface interactions affect the electronic configuration of the corroles, which in turn will help understand the shift in ORR potentials. It is important to emphasize that the $CF_3$-corrole is much more compact than the tpf-corrole, and has a less elaborate Π system, which may also help in facilitating the formation of the strong surface interactions through the surface oxygen moieties on the carbon support.

Apart from the ORR overpotential, the reaction mechanism was also elucidated from the RRDE results. The ORR pathway can either be a direct $4e^-$, consecutive $2 + 2e^-$, or $2e^-$ mechanism. The number of electrons ($n$) transferred during the ORR was calculated using the Levich equation:[31]

$$j_L = (0.201)nFD^{\frac{2}{3}}\omega^{\frac{1}{2}}v^{-\frac{1}{6}}C$$

where $j_L$ is the limiting current density, $D$ and $C$ are the oxygen diffusion coefficient ($2 \times 10^{-5}$ cm$^2$ s$^{-1}$)[32] and bulk concentration of oxygen ($1.2 \times 10^{-6}$ mol cm$^{-3}$), respectively, $\upsilon$ is the kinematic viscosity of the solution (0.01 cm$^2$ s$^{-1}$),[33] and $\omega$ is the rotation speed (rpm).

The number of transferred electrons at 0.4 V *vs.* RHE was calculated and found to be 3.06 and 3.67 for $CF_3$-corrole and tpf-corrole, respectively. The tpf-corrole has a higher tendency for the $4e^-$ pathway, but both seem to follow the $2 + 2e^-$ pathway, since relatively high levels of peroxide anion were detected at the ring electrode (25–40%), as shown in Fig. 2.

To shed more light on the ORR mechanism with the $CF_3$-corrole, the amount of $HO_2^-$ formed during the reaction was

 

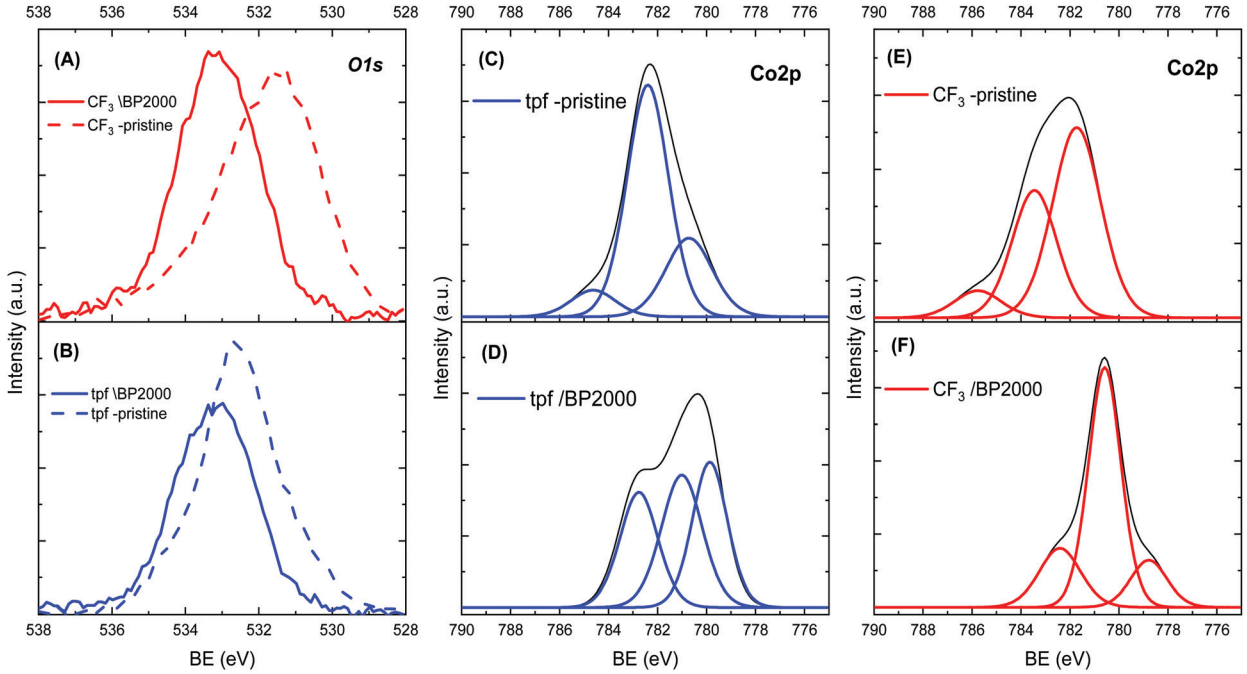


Fig. 3 XPS spectra of (A) O1s of the Co(III)-$CF_3$-corrole before and after incorporation in BP2000, (B) O1s of the Co(III)-tpf-corrole before and after incorporation in BP2000, (C) Co2p spectra of Co(III)-tpf-corrole, (D) Co2p of the Co(III)-tpf-corrole after incorporation in BP2000, (E) Co2p spectra of Co(III)-$CF_3$-corrole, and (F) Co2p of the Co(III)-$CF_3$-corrole after incorporation in BP2000.

quantified, and the number of electrons transferred during the ORR was calculated from it according to the following equations:[34]

$$\%HO_2^- = \frac{I_{ring}}{I_{disk} \cdot 0.37} \times 100 \quad (1)$$

$$n = 2 \cdot \frac{I_{ring}}{I_{disk} \cdot 0.37} + 4 \cdot \left(1 - \frac{I_{ring}}{I_{disk} \cdot 0.37}\right) \quad (2)$$

The results of these calculations over a wide range of voltages are presented in Fig. 4. They support the conclusions from the calculation using the Levich equation, and confirm that the ORR follows the 2 + 2e$^-$ reduction pathway with both corroles.[35] The difference between the electron number calculated from the Levich equation and eqn (2) can be explained by the electrode roughness, which may have an effect on the surface area of the electrode, which is used in the Levich equation.[36] Another possible reason might be related to the $HO_2^-$ that is stranded in the carbon-pores and possibly continues its reduction to $H_2O$ through a disporportionation reaction. While the $CF_3$-corrole maintains a relatively stable $n$ value, the $n$ value of the tpf-corrole increases significantly with the increase of the overpotential. This suggests that the tpf-corrole is a bit more active in the reduction of peroxide anion to hydroxide at high overpotentials.

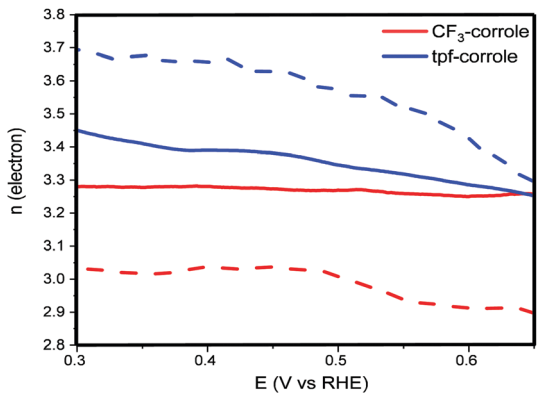


Fig. 4 $n$ electron obtained from eqn (2) (solid line) and Levich equation (dashed line).

In pervious papers, we compared different structural aspects of metallocorrole to elucidate their effect on the ORR electrocatalysis and concluded that once adsorbed in high surface area carbon supports, the corrole substituent has no effect on the ORR overpotential. In order to prove this conclusion, we studied the most compact corrole available. Herein, we compared the well-studied Co(III) tpf-corrole and the contracted structure Co(III) $CF_3$-corrole. We found that in contrast to the previous conclusion, lower overpotentials can be reached by using a less elaborate structure, which allows the formation of strong surface interactions with the support material. The new, compact Co(III) $CF_3$-corrole shows a significant improvement in terms of overpotential. The Co–O binding energy differences, before and after the corroles were adsorbed on BP2000, hint at surface interactions between the corroles and the support. There is a correlation between the larger shift in the XPS spectra and the shift in the ORR overpotentials. Stronger surface interaction translated to higher ORR potentials. It seems that the surface interactions are facilitated through quinone-like moieties on the BP2000 surface. The reaction mechanism

of both corroles is a consecutive 2 + 2e$^-$ reduction, where the tpf-corrole seems to be a better catalyst for peroxide anion reduction. The unique interactions observed with the Co(III) $CF_3$-corrole incorporated in BP2000 advocate further investigation of this phenomena using in-depth computational study, in order to elucidate the effect of the surface interactions on the electron density and the Co(III) $CF_3$-corrole's affinity to oxygen.

The authors would like to thank the Israeli Ministry of Energy and The Fuel Choices and Smart Mobility Initiative at the Israeli Prime Minister's Office for funding this work. One of the authors, A. F., would like to thank the Israeli Ministry of Energy for his fellowship. This work was conducted in the framework of the Israeli Fuel Cells Consortium (part of Israel National Center for Electrochemical Propulsion).

## Conflicts of interest

There are no conflicts to declare.

## Notes and references

1 R. Moliner, M. J. Lázaro and I. Suelves, *Int. J. Hydrogen Energy*, 2016, **41**, 19500–19508.
2 J. Zhang, *PEM fuel cell electrocatalysts and catalyst layers: fundamentals and applications*, Springer Science & Business Media, 2008.
3 L. Elbaz, G. Wu and P. Zelenay, in *Electrocatalysis in Fuel Cells*, ed. M. Shao, Springer, London, 2013, ch. 8, vol. 9, pp. 213–246.
4 V. Mehta and J. S. Cooper, *J. Power Sources*, 2003, **114**, 32–53.
5 J. Van Mierlo, G. Maggetto and P. Lataire, *Energy Convers. Manage.*, 2006, **47**, 2748–2760.
6 O. Lori and L. Elbaz, *Catalysts*, 2015, **5**, 1445–1464.
7 R. Jasinski, *Nature*, 1964, **201**, 1212.
8 R. Othman, A. L. Dicks and Z. Zhu, *Int. J. Hydrogen Energy*, 2012, **37**, 357–372.
9 N. Zion, A. Friedman, N. Levy and L. Elbaz, *Adv. Mater.*, 2018, **30**, 1800406.
10 N. Levy, O. Lori, S. Gonen, M. Mizrahi, S. Ruthstein and L. Elbaz, *Carbon*, 2020, **158**, 238–243.
11 J. S. Shpilman, A. Friedman, N. Zion, N. Levy, D. T. Major and L. Elbaz, *J. Phys. Chem. C*, 2019, **123**, 30129–30136.
12 A. Friedman, I. Saltsman, Z. Gross and L. Elbaz, *Electrochim. Acta*, 2019, **310**, 13–19.
13 M. Kosa, N. Levy, L. Elbaz and D. T. Major, *J. Phys. Chem. C*, 2018, **122**, 17686–17694.
14 A. Friedman, L. Landau, S. Gonen, Z. Gross and L. Elbaz, *ACS Catal.*, 2018, **8**, 5024–5031.
15 N. Levy, A. Mahammed, A. Friedman, B. Gavriel, Z. Gross and L. Elbaz, *ChemCatChem*, 2016, **8**, 2832–2837.
16 H. C. Honig, C. B. Krishnamurthy, I. Borge-Durán, M. Tasior, D. T. Gryko, I. Grinberg and L. Elbaz, *J. Phys. Chem. C*, 2019, **123**, 26351–26357.
17 N. Levy, A. Mahammed, M. Kosa, D. T. Major, Z. Gross and L. Elbaz, *Angew. Chem., Int. Ed.*, 2015, **54**, 14080–14084.
18 N. Levy, J. S. Shpilman, H. C. Honig, D. T. Major and L. Elbaz, *Chem. Commun.*, 2017, **53**, 12942–12945.
19 R. Z. Snitkoff, N. Levy, I. Ozery, S. Ruthstein and L. Elbaz, *Carbon*, 2019, **143**, 223–229.
20 L. Elbaz, E. Korin, L. Soifer and A. Bettelheim, *J. Phys. Chem. Lett.*, 2009, **1**, 398–401.
21 N. Zion, D. A. Cullen, P. Zelenay and L. Elbaz, *Angew. Chem., Int. Ed.*, 2020, **59**, 2483–2489.
22 N. D. Leonard, S. Wagner, F. Luo, J. Steinberg, W. Ju, N. Weidler, H. Wang, U. I. Kramm and P. Strasser, *ACS Catal.*, 2018, **8**, 1640–1647.
23 D. Malko, A. Kucernak and T. Lopes, *Nat. Commun.*, 2016, **7**, 13285.
24 Q.-C. Chen, M. Soll, A. Mizrahi, I. Saltsman, N. Fridman, M. Saphier and Z. Gross, *Angew. Chem., Int. Ed.*, 2018, **57**, 1006–1010.
25 A. Mahammed, I. Giladi, I. Goldberg and Z. Gross, *Chem. – Eur. J.*, 2001, **7**, 4259–4265.
26 V. A. Adamian, F. D'Souza, S. Licoccia, M. L. Di Vona, E. Tassoni, R. Paolesse, T. Boschi and K. M. Kadish, *Inorg. Chem.*, 1995, **34**, 532–540.
27 K. Sudhakar, A. Mahammed, N. Fridman and Z. Gross, *Dalton Trans.*, 2019, **48**, 4798–4810.
28 K. M. Kadish and M. M. Morrison, *Bioinorg. Chem.*, 1977, **7**, 107–115.
29 K. Artyushkova, S. Levendosky, P. Atanassov and J. Fulghum, *Top. Catal.*, 2007, **46**, 263–275.
30 L. Elbaz, E. Korin, L. Soifer and A. Bettelheim, *J. Electrochem. Soc.*, 2010, **157**, B27–B31.
31 J. Nikolic, E. Expósito, J. Iniesta, J. González-Garcia and V. Montiel, *J. Chem. Educ.*, 2000, **77**, 1191.
32 R. Davis, The Solubility and Diffusion Coefficient of Oxygen in Potassium Hydroxide Solutions, *Electrochim. Acta*, 1967, **12**, 287–297.
33 W. Robert, *Handbook of chemistry and physics*, CRC Press, 1988.
34 A. J. Bard, L. R. Faulkner, J. Leddy and C. G. Zoski, *Electrochemical methods: fundamentals and applications*, Wiley, New York, 1980.
35 K. M. Kadish, L. Frémond, Z. Ou, J. Shao, C. Shi, F. C. Anson, F. Burdet, C. P. Gros, J.-M. Barbe and R. Guilard, *J. Am. Chem. Soc.*, 2005, **127**, 5625–5631.
36 A. J. Bard, *Integrated chemical systems: a chemical approach to nanotechnology*, Wiley, New York, 1994.



 